AD-A112 598 CALIFORNIA UNIV LOS ANGELES CENTER FOR PLASMA PHYSIC--ETC F/6 20/14
BEAT EXCITATION OF WHISTLER WAVES,(U)
JAN 82 M SHOUCRI, G J MORALES, J E MAGGS N00014-75-C-0476
UNCLASSIFIED PPG-609 NL

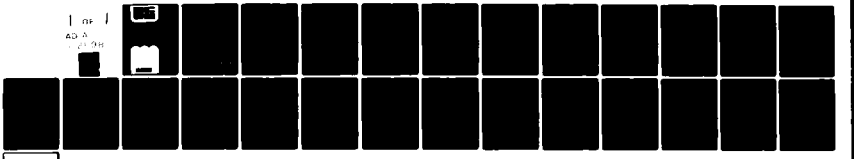

END
DATE FILMED
04-82
DTIC

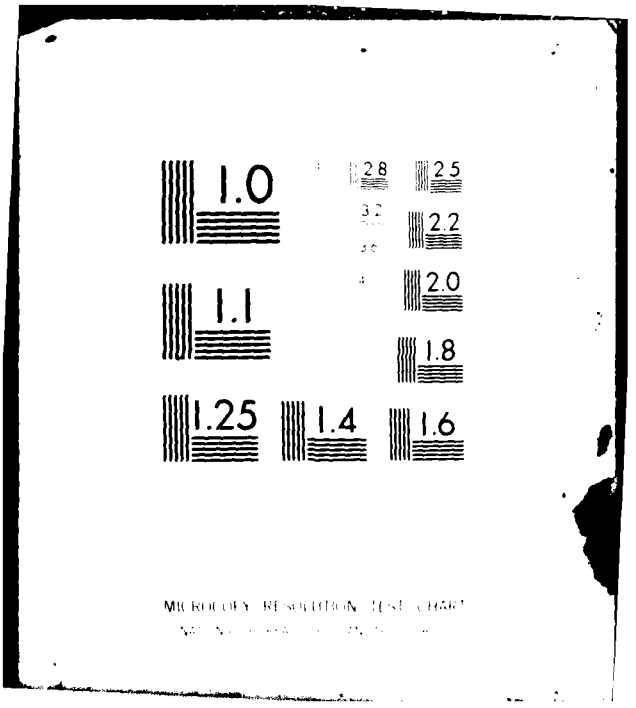
1.0
2.8
2.5
3.2
2.2
2.0
1.1
1.8
1.25
1.4
1.6
MICROCOPY RESOLUTION TEST CHART

(2)

CENTER FOR
PLASMA PHYSICS
AND
FUSION ENGINEERING

UNIVERSITY OF CALIFORNIA
LOS ANGELES

(2)

Beat Excitation of Whistler Waves

M. Shoucri, G. J. Morales & J. E. Maggs

PPG-609 January, 1982
CONTRACT N0001 4-75-C-0476

Department of Physics
University of California
Los Angeles, California 90024

1. Introduction

In studies of wave propagation in magnetized plasmas it is often of interest to excite low frequency modes from a remote location under controllable conditions. These modes can be used for a variety of purposes, e.g., as a tool for diagnosing plasma properties,[1] to provide a seed for growth of low frequency turbulence,[2,3] or perhaps to establish a low frequency communications link, as may be the case in the ionosphere.[4-6] Regardless of the particular application, a common problem is that at low frequencies it is difficult to excite an external electromagnetic signal that penetrates deeply into the plasma where the propagation of the low frequency mode is desired. For this reason one is lead to consider processes in which the low frequency mode is indirectly excited by energy sources which penetrate the plasma more readily. Two obvious choices are particle streams and high frequency waves. As is well known, both of these sources can trigger a variety of parametric instabilities whose decay channels can coincide with the desired low frequency mode. An intrinsic drawback of the parametric excitation scheme is that the amplitude and phase of the low frequency mode cannot be controlled by the experimentalist, and are difficult to predict theoretically. Essentially, because the saturation of the instability is the result of complicated nonlinear interactions.

A more controllable process consists of beating two high frequency pump waves of frequency ω_1 and ω_2 to drive a low frequency mode at $\omega = \omega_1 - \omega_2$, resonantly. In this process the power transferred to the low frequency mode depends on the product of the individual pump powers, and as is illustrated in this study, the transfer coefficient can be calculated from first principles. In addition, the strict constraint imposed by the resonance criterion permits the localization of the excitation region. Although the

general idea of beat excitation can be applied to various plasma modes,[7-11] the majority of previous theoretical studies have considered the generation of electrostatic modes in plasmas which are transparent to the pump waves. Here we consider a problem in which the existence of the plasma nonuniformity is advantageously used to localize the generation of an electromagnetic wave in the whistler regime.

The geometry of the problem is sketched in Figure 1. Two high frequency electromagnetic waves, at closely spaced frequencies ω_1 and ω_2, are launched from vacuum into a magnetized plasma along the direction of the zero order density gradient ∇N_o. In this work we concentrate primarily on the case where the static magnetic field $\underline{B}_o$ points against ∇N_o, i.e., $-B_o \,||\, \nabla N_o$. This choice allows ready comparison with ongoing experiments performed in the northern auroral ionosphere.[12] The vacuum polarization of the electromagnetic waves is chosen to be left-handed in order to avoid excitation of unwanted electrostatic nonlinear phenomena near the plasma resonance, i.e., at $\omega_p = \omega_j$, where ω_p is the local electron plasma frequency and $j = 1,2$. Each electromagnetic wave penetrates into the plasma up to its left-hand cut-off layer, i.e., where $\omega_p^2 = \omega_j(\omega_j - \Omega)$, with Ω the electron gyrofrequency and it is assumed that $\omega_j > \Omega$. At this location each wave is reflected and exhibits an Airy function standing wave pattern. The two Airy patterns are shifted with respect to each other because they are centered about different reflection layers. It is this shift of the two patterns that produces a spatially localized interaction pattern oscillating at the beat frequency $\omega = \omega_1 - \omega_2$ with a characteristic k_z spectrum, where k_z is the wavenumber along $\underline{B}_o$. The essential idea is this excitation scheme consists of adjusting the various free parameters such that the k_z corresponding to a whistler at $\omega_1 - \omega_2$ falls as closely as possible to the spectral peak associated with the beat of the individual Airy patterns. Physically, the idea is to generate a matched

antenna inside the plasma near the location defined by $\omega_p^2 = \omega_j(\omega_j - \Omega)$. The possibility of matching to a whistler is greatly facilitated because this mode exhibits a dispersion relation which is essentially constant over the region where the beat antenna is formed.

A semi-quantitative criterion for the feasibility of generating a matched antenna in a plasma can be obtained as follows. Near the reflection layer of the j^{th} electromagnetic wave the Airy pattern exhibits an effective wavenumber $k_A \sim (k_j L)^{2/3}/L$ where $k_j = \omega_j/c$, with c the speed of light and L the density gradient scale length. Since $\omega/\omega_j << 1$, the beat interaction pattern has a significant spectral amplitude at a fraction of k_A. Equating the wavenumber of the whistler wave k_z with k_A and using the whistler dispersion relation $k_z = (\omega_p^2/\omega\Omega)^{1/2}(\omega/c)$ results in the condition

$$\frac{\omega}{\Omega} \sim (k_j L)^{-2/3} \tag{1}$$

where it is assumed that $\omega_j^2 \sim \omega_p^2 >> \Omega^2$. Equation (1) indicates that in plasmas in which the density gradient is sufficiently large it is possible, in principle, to use beat excitation to resonantly excite a low frequency whistler, i.e., $\omega/\Omega << 1$. For instance, in the ionosphere $k_j L \sim 10^3$, $\Omega/2\pi \sim 1.4$ MHz, hence Eq. (1) shows the beat coupling to waves in the 10 kHz range is possible. In a laboratory plasma with an attainable $k_j L \sim 10^2$ and $|\underline{B}_o| \sim 400$G coupling to whistlers at $\omega/2\pi \sim 50$ MHz is expected.

Although the most efficient coupling to a whistler mode is accomplished by an oscillating current perpendicular to $\underline{B}_o$, i.e., magnetic multipole excitation, such a current cannot be directly generated by the beat of two high frequency waves propagation along $\underline{B}_o$. Therefore, in this geometry coupling is accomplished through the less efficient electric dipole excitation due to the generation of a beat electric field along $\underline{B}_o$. The aim of this study is to

calculate the coupling coefficient for this process taking into consideration the important effects of plasma nonuniformity.

The beat electric field along $\underline{B}_o$ arises due to the charge separation produced by the beat ponderomotive force acting on the plasma electrons. The weak but finite variation of the high frequency pumps across $\underline{B}_o$, i.e., finite spot size at the reflection layer, provides the necessary coupling to a slightly oblique whistler. The transverse wavenumber spectrum of the beam spot at the reflection layer defines the spectrum of oblique whistlers radiated by the beat antenna.

The theoretical description of whistler mode excitation by the beat of two high frequency pumps requires three separate calculations: 1) a suitable representation of whistler mode properties, 2) calculation of nonlinear beat coupling, i.e., the source term for the whistler wave equation, 3) radiation of whistler using appropriate source functions in a nonuniform plasma. Next we proceed to discuss each of these calculations in Section II. A discussion of the results is given in Section III.

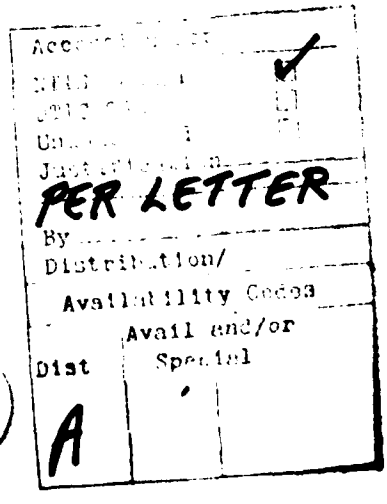

II. Theory

First we proceed to describe the whistler mode generated by the beat excitation process. A simplifying but realistic assumption is that the dispersion properties of the whistler mode can be obtained by assuming that the plasma density is constant and equal to the density n_o at the reflection layer of the high frequency waves. This is justifiable because the whistler mode is far from any cut-off or resonance, and for the plasmas of interest $k_\perp L \gg 1$ while the beat frequency antenna is effective over spatial scales of the order of $2\pi/k_z$. The whistler wave at frequency ω propagates at a small angle relative to $\underline{B}_o$ with a wavenumber $\underline{k} = \underline{k}_\perp + k_z\hat{\underline{z}}$, where $\underline{k}_\perp = k_x \hat{\underline{x}} + k_y \hat{\underline{y}}$ with $k_\perp = (k_x^2 + k_y^2)^{1/2} \ll |k_z|$. Since $k_\perp$ is fixed by the finite transverse dimension of the high frequency beams, k_z is determined self-consistently from the plasma dispersion relation at frequency ω.

Using the cold plasma fluid equations together with Maxwell's equations yields the following differential equations which determine the spatial dependence of the whistler electric field

$$k_o^{-2} \frac{d^2E^\pm}{dz^2} + [\varepsilon^\pm - \frac{1}{2}(k_\perp/k_o)^2]E^\pm = \frac{1}{2}[\frac{k_y \pm ik_x}{k_o}]^2 E^\mp \pm [(k_y \pm ik_x)/2k_o^2] \frac{dE_z}{dz} , \quad (2)$$

$$[\varepsilon_{\prime\prime} - (k_\perp/k_o)^2]E_z = [(k_y+ik_x)/k_o^2] \frac{dE^-}{dz} - [(k_y-ik_x)/k_o^2] \frac{dE^+}{dz} , \quad (3)$$

where $E^\pm(z) = (E_x \mp iE_y)/2$, $\varepsilon^\pm = 1 - (\omega_{po}/\omega)^2 [1 \pm (\Omega/\omega)]^{-1}$, $\varepsilon_{\prime\prime} = 1 - (\omega_{po}/\omega)^2$, $k_o = \omega/c$, E_x and E_y are the x and y components of the electric field, ω_{po} is the electron plasma frequency at the reflection layer, and a time dependence $\exp(-i\omega t)$ is assumed. The plus and minus superscripts refer to the right- and left-handed polarizations, respectively. The z dependence is retained in Eqs. (2) and (3) in order to incorporate the dipole field generated by the beat frequency antenna. For small angles of propagation relative to the magnetic

field lines, one obtains from Eq. (2) the approximate whistler dispersion relation

$$(k_z/k_o)^2 \simeq \varepsilon^{\pm} \simeq \mp \omega_{po}{}^2/\omega\Omega, \tag{4}$$

which is seen to be insensitive to $k_\perp$. The quantity $\omega_{po}{}^2/\omega\Omega$ is much larger than unity, and the propagating mode in Eq. (4) is associated with the E^- wave while the evanescent mode corresponds to the E^+ wave. The high evanescence of the latter and its weak coupling to the propagating mode allow us to neglect its effect on the propagation of the E^- wave. Incorporating these assumptions, one finds that the whistler mode behavior is governed by the following scaled differential equation,

$$\frac{d^2E^-}{d\zeta^2} + b^2E^- = S, \tag{5}$$

where $b^2 = \varepsilon^- - \frac{1}{2}(k_\perp/k_o)^2 \simeq \omega_{po}{}^2/\omega\Omega$, $\zeta = k_o z$,

$$S = -[(k_y - ik_x)/2k_o]\,\frac{dE_s}{d\zeta}\,. \tag{6}$$

The source term S arises from the generation of an ambipolar electric field $\underline{E}_s$ due to the beat ponderomotive force produced by the high frequency pumps. This effect is calculated next.

As already stated in Sec. I, the relevant nonlinearity in the problem is the beat of the two high frequency pumps near their reflection layers. The lowest order nonlinear effects occur at zero frequency (d.c.), at low frequency $\omega = \omega_1 - \omega_2$, and at high frequencies $\omega_1 + \omega_2$, $2\omega_1$, $2\omega_2$. The zero frequency effect is produced by the self-modulation of each wave, giving rise to a modification of the zero order density profile which we do not include in the present calculation. The high frequency sideband at $\omega_1 + \omega_2$ as well as the harmonics $2\omega_1$, $2\omega_2$ are unable to excite a wave because the

spatial interaction pattern does not provide a suitable k_z match, as is possible for the whistler wave at $\omega_1 - \omega_2$.

The nonlinearity at $\omega = \omega_1 - \omega_2$ can be obtained from the electron fluid equation of motion by iteration. First one neglects the nonlinear effects and calculates the high frequency response of the electrons to each pump separately

$$\underline{v} = \underline{v}_1 \exp(-i\omega_1 t) + \underline{v}_2 \exp(-i\omega_2 t), \tag{7}$$

where $\underline{v}_j = \underline{\mu}_j \cdot \underline{E}_j$, $j = 1, 2$, and

$$\underline{\mu}_j = \frac{-ie}{m\omega_j(1-Y_j^2)} \begin{pmatrix} 1 & +iY_j & 0 \\ -iY_j & 1 & 0 \\ 0 & 0 & 1-Y_j^2 \end{pmatrix}, \tag{8}$$

with $Y_j = \Omega/\omega_j$, and e and m are the electron charge and mass. The nonlinear effect is calculated by inserting the linearized velocities into the averaged force equation. This yields a ponderomotive force oscillating at frequency ω acting on the electrons and given by

$$\underline{F} = - n_o[m(v_{1z} \frac{d}{dz} \underline{v}_2^* + v_{2z}^* \frac{d}{dz} \underline{v}_1) + \frac{e}{c}(\underline{v}_1 \times \underline{B}_2^* + \underline{v}_2^* \times \underline{B}_1)], \tag{9}$$

where $\underline{B}_j$ is the magnetic field of wave j. We choose to excite both pump waves with left-handed circular polarization to avoid additional effects at $\omega_p = \omega_j$. The appropriate representation of the pump electric field is then E_j^-, defined in a manner similar to the field of the whistler wave. Using Faraday's law to eliminate $\underline{B}_j$ yields

$$\underline{F} = - \hat{z} \frac{2n_o e^2}{m\omega_1\omega_2} [\frac{1}{(1-Y_1)} E_1^- \frac{d}{dz} E_2^{-*} + \frac{1}{(1-Y_2)} E_2^{-*} \frac{d}{dz} E_1^-] \exp(-i\omega t), \tag{10}$$

where it is seen that the force points along the density gradient ∇N_o, and

that both pumps have symmetrical contribution, as expected. The effect of this force is to produce an ambipolar electric field oscillating at ω whose self-consistent strength is found as follows.

The low frequency electron equation of motion takes the form

$$m \frac{d\underline{u}_e}{dt} = -e \underline{E}_s + \underline{F}/n_o, \tag{11}$$

where $\underline{u}_e$ is the low frequency component of the electron velocity, and $\underline{E}_s$ is the self-consistent ambipolar field which also acts on the ions of mass M, charge q, and velocity $\underline{u}_i$ through

$$M \frac{d\underline{u}_i}{dt} = q \underline{E}_s \quad , \tag{12}$$

where the effect of the ion ponderomotive force is neglected because of the large inertia of the ions and it is also assumed that $\omega >> \Omega_i$ (i.e., negligible resonance enhancement from the ion gyrofrequency Ω_i). Solving for the linearized velocities from Eqs. (11) and (12) and using the continuity equations together with Poisson's equation yields

$$\underline{E}_s = \frac{-(\omega_{po}/\omega)^2}{n_o e \epsilon_s} \underline{F} \tag{13}$$

where $\epsilon_s = 1 - (\omega_{po}/\omega)^2 - (\omega_{pi}/\omega)^2$, ω_{pi} is the ion plasma frequency, and characteristically $(\omega_{pi}/\omega)^2 << 1$.

It is now possible to use Eqs. (10) and (13) to obtain the source term S in Eq. (6)

$$S(k_x, k_y, \zeta) = \frac{-eE_{01}E_{02}(k_y - ik_x) f(k_x, k_y) (\omega_{po}/\omega)^2}{m\omega_1\omega_2\epsilon_s} \frac{d}{d\zeta} \left[\frac{1}{1-Y_1} \psi_1 \frac{d}{d\zeta} \psi_2^* + \frac{1}{1-Y_2} \psi_2^* \frac{d\psi_1}{d\zeta} \right] \tag{14}$$

where the amplitude of each pump field is expressed as

$$E_j(x, y, \zeta) = E_{oj} f_j(x,y)\psi_j(\zeta). \tag{15}$$

The quantity E_{oj} corresponds to the electric field amplitude of wave j at at its reflection layer, and the function $f(k_x,k_y)$ in Eq. (14) is the Fourier transform of the product of the transverse envelopes of each pump beam, i.e., $f_j(x,y)$ in Eq. (15). A typical functional dependence is $f_j(x,y) = \exp[-(x^2+y^2)/d^2]$ with $k_z d \gg 1$, and $k_\perp \sim 2/d$.

To completely determine the spatial dependence of the source term S we need to find the functions $\psi_j(\zeta)$, i.e., the wave equations for the high frequency pumps need to be solved near their respective reflection layer. This is easily done in the relevant limit $k_\perp/k_j \ll 1$, which gives

$$k_j^{-2} \frac{d^2}{dz^2} \psi_j(z) + \left[1 - \frac{\omega_p^2(z)}{\omega_j^2(1-Y_j)}\right] \psi_j(z) = 0, \tag{16}$$

where the explicit spatial dependence of the density profile is indicated. We take this variation to be essentially linear near the reflection layer, i.e., we choose

$$1 - \frac{\omega_p^2(z)}{\omega_j^2(1-Y_j)} \simeq - \frac{z}{L}, \tag{17}$$

with $z = 0$ corresponding to the reflection layer of the higher frequency pump ω_1. Substituting Eq. (17) in Eq. (16) gives the Airy differential equation. After scaling the spatial variable in the equation of pump 2 to that in the equation of pump 1, one obtains the solutions

$$\psi_1(\xi) = \mathrm{Ai}(\xi), \tag{18}$$

$$\psi_2(\xi) = \mathrm{Ai}(\xi + \Lambda), \tag{19}$$

where $\xi = (k_1 L)^{2/3}(z/L)$, $\Lambda = (k_1 L)^{2/3}[(1-Y_1) - (\omega_2/\omega_1)^2(1 - Y_2)]$, and Ai refers to the Airy functions. These solutions are valid in the neighborhood

of the cut-off for the left wave. Using Eqs. (18) and (19) in Eq. (14) determines the source term completely.

The next task consists of solving Eq. (5) with the given source S to determine the amplitude of the whistler waves excited by the beat frequency antenna. Using the Green's function method yields

$$E^{-}(k_x, k_y, \zeta) = -\frac{(k_y - ik_x)}{4k_o}\{\exp(ib\zeta)\int_{-\infty}^{\zeta} d\zeta' E_s(\zeta')\exp(-ib\zeta') - \exp(-ib\zeta)\int_{\zeta}^{\infty} d\zeta' E_s(\zeta')\exp(ib\zeta')\}, \tag{20}$$

from which the asymptotic fields are found to be

$$E^{-}(k_x, k_y, \zeta) \sim \alpha(\pm\infty)\exp(\pm ib\zeta), \qquad \zeta \to \pm\infty \tag{21}$$

where

$$\alpha(\pm\infty) = \pm a\int_{-\infty}^{\infty} d\xi \left[\frac{1}{1-Y_1}\mathrm{Ai}(\xi)\,\mathrm{Ai}'(\xi+\Lambda) + \frac{1}{1-Y_2}\mathrm{Ai}(\xi+\Lambda)\mathrm{Ai}'(\xi)\right]\exp(\pm iK\xi), \tag{22}$$

$$a = \frac{-(\omega_{po}/\omega)^2}{\epsilon_s}\,\frac{(k_y - ik_x)f(k_x,k_y)}{2}\left(\frac{eE_{01}E_{02}}{m\omega_1\omega_2}\right), \tag{23}$$

$$K = bk_oL/(k_1L)^{2/3},$$

and the prime means a derivative with respect to ξ. Recalling the assumption that $\Omega/\omega_j \ll 1$, this implies that $(1 - Y_1) \simeq (1 - Y_2)$, hence the two terms in the integrand of Eq. (22) have nearly identical coefficients and this allows us to approximate Eq. (22) by

$$\alpha(\infty) \simeq \frac{iKa}{1-Y_1} I, \tag{24}$$

where

$$I = \int_{-\infty}^{\infty} d\xi\, \mathrm{Ai}(\xi)\,\mathrm{Ai}(\xi+\Lambda)\exp(-iK\xi). \tag{25}$$

To obtain $\alpha(-\infty)$, I is replaced by its complex conjugate.

Since the Airy functions are not square integrable in the interval $(-\infty, 0)$, the Fourier transform integral I is not well defined. The difficulty arises as $\xi \to -\infty$ where the function Ai oscillates rapidly but its amplitude decays slowly. This behavior results from our usage of the Airy function solutions away from the neighborhood of the turning points. Since the antenna oscillating at the beat frequency is produced by the interaction of the main lobes of the Airy patterns within a distance of a few whistler wavelengths $(2\pi/k_z)$, the difficulty introduced by the highly oscillatory tail is easily overcome by introducing in the integrand of Eq. (25) a weight function $w(\xi) = \exp(-\xi^2/4\Lambda^2)$ which is nearly constant over the important interaction region and cancels the slowly decaying unphysical behavior of the tail as $\xi \to -\infty$. Other choices for $w(\xi)$ have been tried and the results are found to be relatively insensitive to the particular form used. To illustrate the spatial dependence of the beat frequency antenna field generated by the pump waves, a plot of the function $Ai(\xi)Ai(\xi + \Lambda)w(\xi)$ is shown in Fig. 2 for a choice of $\Lambda = 10$. The arrows at ω_1 and ω_2 indicate the turning points for each pump, and the pure sinusoidal wave at the top of the figure represents the wavelength of the excited whistler. The normalized k_z spectrum of the antenna is shown in Fig. 3, where the arrows indicate the corresponding wavenumbers of the excited whistlers; only those wavenumbers satisfying the whistler wave dispersion relation of Eq. (4) are allowed to propagate. The ordinate represents the magnitude of the integral I and the two sidebands correspond to the two possible excitation directions of the whistlers for each given value of $k_\perp$. Since it is expected that the transverse beam spot is axially symmetric in $k_\perp$, the antenna radiates the whistler waves along a cone whose axis is along the z-axis and whose half-angle is given by $\tan^{-1}(k_\perp/k_z)$ as sketched

in Figure 1.

Once the frequency of one of the pumps is chosen, and the radiated whistler is selected then, for a given density scale length L, both K and Λ are uniquely determined. This is shown in Fig. 4 where both K and Λ are plotted versus the whistler frequency for fixed values of $\omega_1/2\pi$ and L corresponding here to the case of ionospheric plasmas. The process of fixing Λ also determines, independently of K, the interaction pattern of Fig. 2 and its spectrum in Fig. 3. The most efficient coupling occurs when the value of K shown in Fig. 4 coincides with the maxima of the spectrum curve shown in Fig. 3. Although there is no a priori reason for the value of K to be close to the spectral peak of the antenna, it turns out that for parameters typical of ionospheric and laboratory plasmas it is possible to approach the optimum value, as exemplified by the arrows in Figure 3.

Finally, we proceed to calculate the strength of the radiated signal and the efficiency of the coupling between the high frequency pump waves and the whistler wave.

We substitute Eq. (24) into Eq. (21) and take the inverse Fourier transform of the transverse dependence to obtain

$$E^{-}(x,y,z) \sim E_R \exp[i(\pm bk_o z \pm \phi + \theta + \pi/2)], \qquad z \to \pm\infty \tag{26}$$

where

$$E_R = \frac{-(\omega_{po}/\omega)^2}{\varepsilon_s} \frac{2eKE_{01}E_{02}|I|}{m\omega_1\omega_2(1-Y_1)} \frac{\sqrt{x^2+y^2}}{d^2} \exp\,[-2(x^2+y^2)/d^2], \tag{27}$$

ϕ is the phase of I, and $\theta = \tan^{-1}(y/x)$. Equation (27) gives the total amplitude of the radiated field of the whistler wave. A qualitative sketch is shown in Fig. 5. It exhibits a null on the z axis, and a maximum along a circular ring of radius d/2.

The average energy flux radiated in either the positive or negative z direction is given in MKS units by $\frac{1}{2\mu_o}(\underline{E}^- \times \underline{B}^{-*})$, which leads to the following expression for the total power radiated

$$P_R = 2b\sqrt{\epsilon_o/\mu_o} \int_{-\infty}^{\infty}\int_{-\infty}^{\infty} dxdy\ E_R^2$$

$$P_R = 2\pi b\sqrt{\epsilon_o/\mu_o}\ [eKE_{01}E_{02}|I|/2m\omega_1\omega_2(1-Y_1)],^2$$

where ϵ_o and μ_o are the permittivity and permeability of free space, respectively.

Assuming that the pump waves originate from a transmitter in vacuum, one can relate the amplitude E_{oj} to the vacuum pump power P_p through the approximate expression $P_p \simeq \pi d^2\sqrt{\epsilon_o/\mu_o}\ (E_{01}^2 + E_{02}^2)$. The efficiency with which the whistler wave is excited by the pumps is

$$\eta = P_R/P_p. \tag{29}$$

This is a nonlinear efficiency because it depends on the pump power. In order to obtain a more practical expression for η we rewrite Eq. (29) as

$$\eta = \frac{(\omega_{po}/\sqrt{\omega\Omega})\,(eK|I|)^2}{8\pi d^4\sqrt{\epsilon_o/\mu_o}\ [m\omega_1\omega_2(1-Y_1)]^2}\ P_p, \tag{30}$$

where we made the reasonable assumption that $E_{01} = E_{02} = E_o$. Equation (30) gives the coupling efficiency η as a function of the total power radiated by the pump.

III. Discussion

The present calculation provides a clear example of how the nonlinear efficiency for the radiation of a low frequency electromagnetic signal due to the beat of two high frequency pumps can be determined from first principles. The calculation includes plasma nonuniformity as well as finite spatial extent of the pumps. The figure of merit for the beat process is given by the compact expression, shown in Eq. (30). A rough order of magnitude evaluation of this expression shows a radiated power P_R whose dependence on pump power P_p scales as $P_R \sim (v_{os}/c)^2 P_p$, where v_{os} refers to the oscillating velocity of an electron due to the high frequency pump, and c is the speed of light. This dependence illustrates readily the extreme inefficiency of the process at low pump power (i.e., small v_{os}). Another fundamental factor which lowers the efficiency is that the coupling to the whistler wave occurs through electric dipole excitation. The dependence due to this effect appears through the d^{-4} term in Eq. (30).

A more efficient excitation mechanism would be to use magnetic coupling, i.e., to generate a nonlinear transverse current oscillating at the beat frequency ω. However, within the constraints of the present geometry (i.e., $-\underline{B}_o \parallel \nabla N_o$) this more desireable situation cannot be realized directly.

The most advantageous feature of the beat excitation described here is the controllability of the spatial location from which the whistler emanates. By proper adjustment of the pump frequency ω_1 and usage of Fig. 4 in conjunction with Fig. 3 the optimum efficiency can be realized for a desired remote location in the plasma. Due to the dispersive properties of whistlers, the radiated low frequency signal exhibits a characteristic headlight pattern, as is illustrated in Fig. 5. The signal is generated at the reflection layer of the high frequency pumps and is radiated along a hollow cylinder concentric

with the pump beam illumination spot.

Considering parameters typical of the auroral ionosphere, $L \simeq 50$ km, $\Omega/2\pi = 1.4$ MHz, reflection layer at 150 km, and present transmitter capabilities, i.e., $P_p = 5$ MW, $\omega_1/2\pi = 5$ MHz, $\omega_2/2\pi \simeq 4.9$ MHz, and antenna gain of 30 db, results in values of the scaled quantities $K = 4.64$, $\Lambda = 10.3$, and $|I| \simeq 1.4$. These conditions give rise to the radiation of a whistler at $\omega/2\pi \simeq 100$ KHz with an electric field amplitude of 5μV/m at an extremely low nonlinear efficiency level of $\eta \sim 10^{-11}$. In spite of the low system efficiency, present experiments detect signals at comparable levels.[4,6]

It should also be mentioned that naturally occuring atmospheric lightning radiates a broad spectrum of electromagnetic waves. In principle, the high frequency noise waves can trigger the secondary radiation of whistlers by the mechanism described in this work.

For parameters realizable in a large laboratory plasma device, $|\underline{B}_o| = 400$G, $\omega_1/2\pi = 2.8$ GHz, $\omega_2/2\pi = 2.5$GHz, $L \simeq 10$m, one obtains $K = 4.33$, $\Lambda = 11.2$, $|I| \sim 1$, which results in the excitation of a whistler at $\omega/2\pi = 300$ MHz with an electric field amplitude of 50 mV/m at a coupling efficiency of $\eta \sim 10^{-8}$ for an input pump power of 1 KW. Thus, the effect is amenable to experimental investigation.

Finally, it should be noted that if the density gradient points at a small angle θ relative to the magnetic field, then the results described in this study remain valid up to an order $(\Omega/\omega_1)^2 \sin^2\theta$. For ionospheric plasmas this condition restricts the applicability of the present analysis to high latitude auroral plasmas.

References

1. E. S. Weibel, Phys. Fluids 19, 1237 (1976).
2. A. Y. Wong, W. F. Di Vergilio, and K. Iizuka, Phys. Lett. 75A, 144 (1979).
3. M. S. Sodha, Md. Salimullah, and R. P. Sharma, Phys. Rev. A, 21, 1708 (1980).
4. G. G. Getmanstev, N. A. Zuikov, D. S. Kotik, L. F. Mironenko, N. A. Mityakov, V. O. Rapoport, Yu. A. Sazonov, V. Yu. Trakhtengerts, and V. Ya. Eidman, JETP Lett. 20, 101 (1974) [ZhETF Pis. Red. 20, 229 (1974)].
5. T. Turunen, P. S. Cannon, and M. J. Rycroft, Nature 286, 375 (1980).
6. P. Stubbe, H. Kopka, and R. L. Dowden, J. Geophys. Res. 86, 9073 (1981).
7. N. M. Kroll, A. Ron, and N. Rostoker, Phys. Rev. Lett. 13, 83 (1964).
8. B. I. Cohen, A. N. Kaufman, and K. M. Watson, Phys. Rev. Lett. 29, 581 (1972).
9. K. B. Dysthe, E. Mjølhus, and J. Trulsen, Phys. Scr. 21, 122 (1980).
10. K. Rypdal, J. Geophys. Res. 86, 1544 (1981).
11. F. Braun, and G. Lechert, Bull. Am. Phys. Soc. 26, 949 (1981).
12. A. Y. Wong, J. Santoru, and G. G. Sivjee, J. Geophys. Soc. 86, 7718 (1981).

Figure Captions

Fig. 1 Geometry of the problem, where Λ is the scaled separation of the pumps obtained in Eq. (19).

Fig. 2 Spatial pattern of the beat frequency antenna generated by the two high frequency pumps. The arrows show the turning points for each pump which are separated by a scaled distance $\Lambda = 10$. The radiated whistler wavelength is shown on top for reference.

Fig. 3 Normalized k_z spectrum of the antenna pattern shown in Fig. 2. The arrows indicate the magnitude of I corresponding to the wavenumbers of the excited whistlers.

Fig. 4 Normalized whistler wavenumber K and separation of the pumps Λ versus whistler frequency ω for pump frequency $\omega_1/2\pi = 5$ MHZ, and density scalelength L = 50 km.

Fig. 5 Sketch of the radiated whistlers showing the transverse dependence of the amplitude [$\rho = (x^2 + y^2)^{1/2}$].

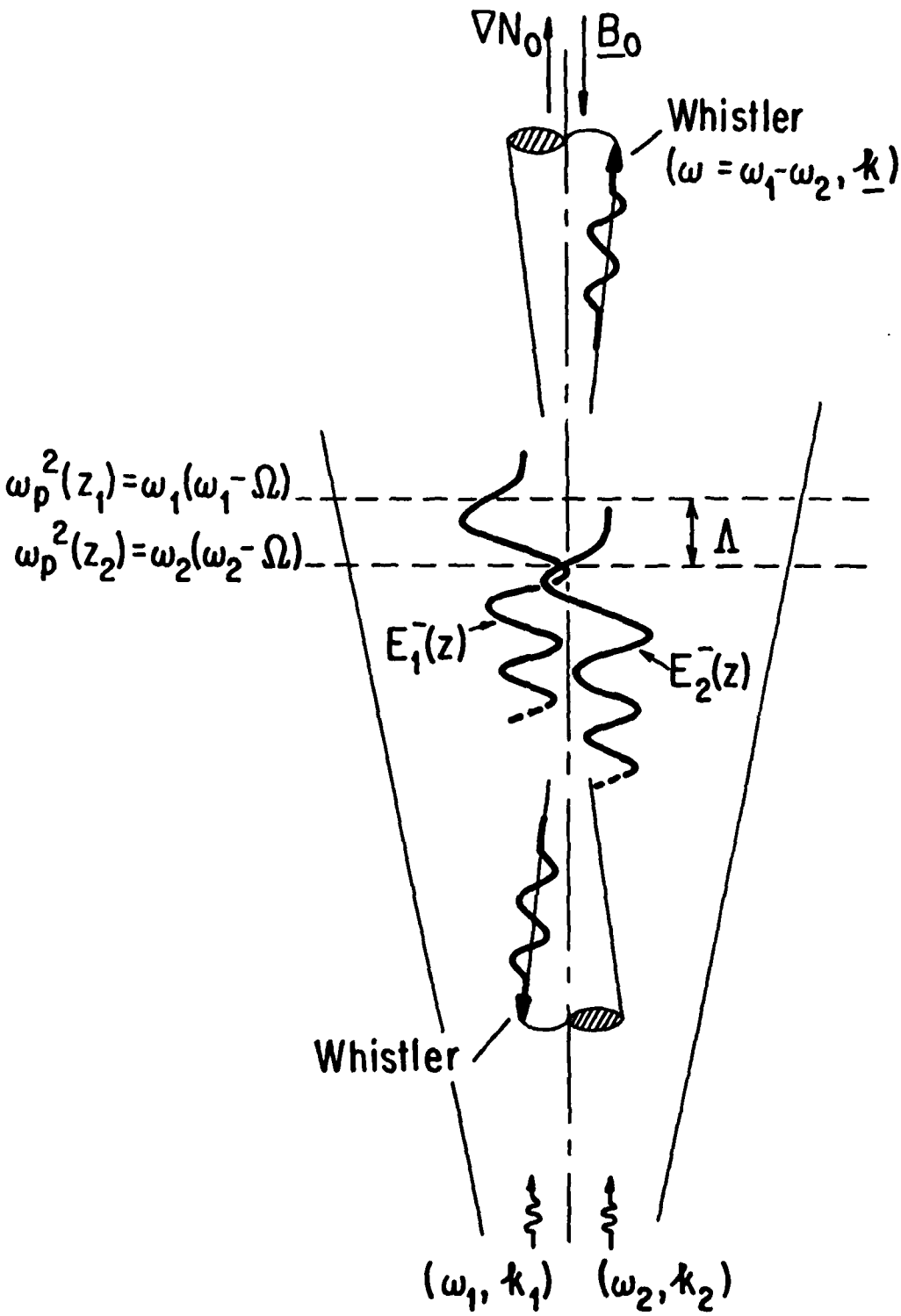
∇N0
B0
Whistler
(ω = ω1-ω2, k)
ωp2(z1)=ω1(ω1-Ω)
ωp2(z2)=ω2(ω2-Ω)
Λ
E1-(z)
E2-(z)
Whistler
(ω1, k1)
(ω2, k2)

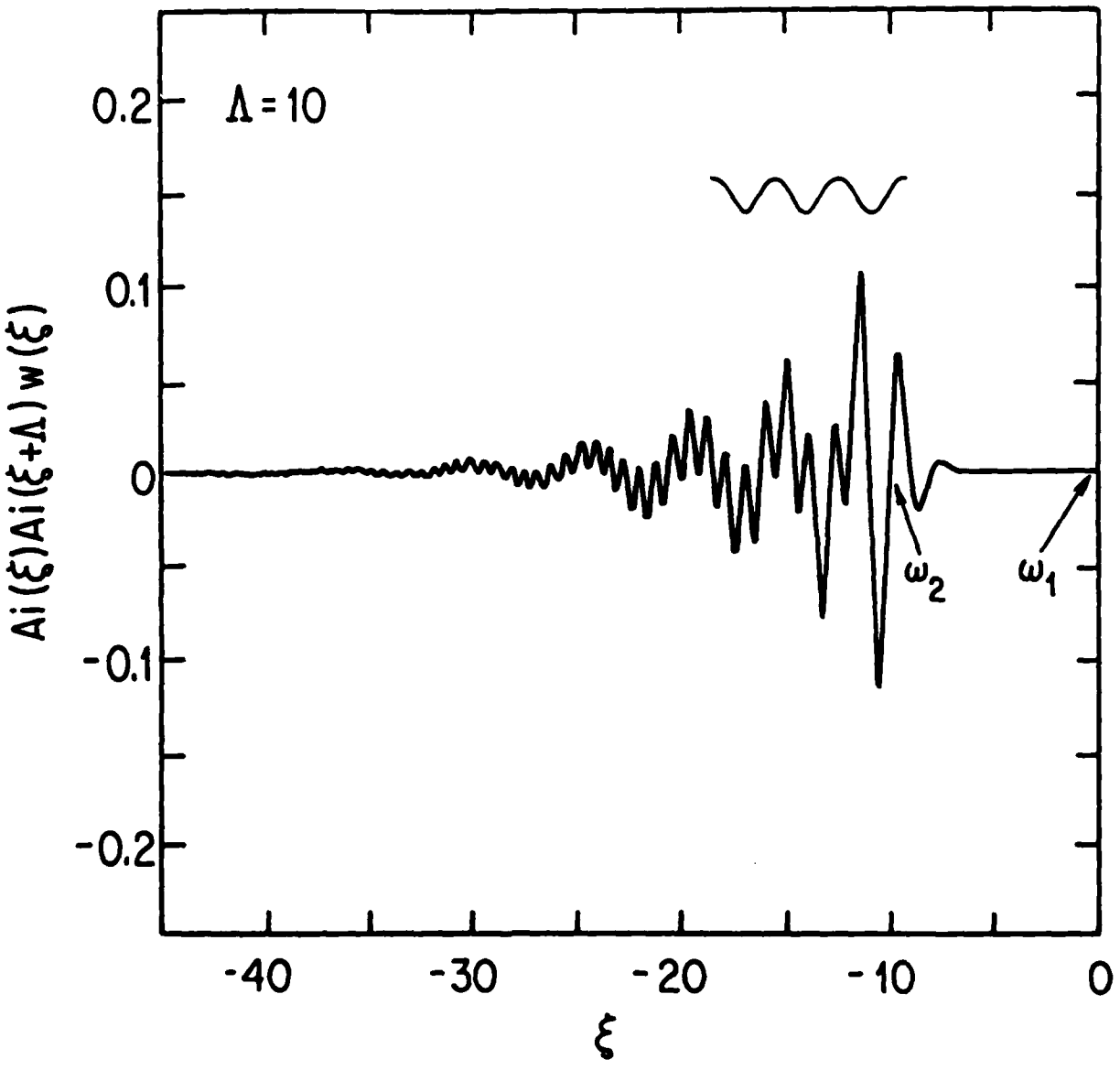
Λ = 10
0.2
0.1
0
-0.1
-0.2
-40
-30
-20
-10
0
ξ
Ai(ξ)Ai(ξ+Λ) w(ξ)
ω2
ω1

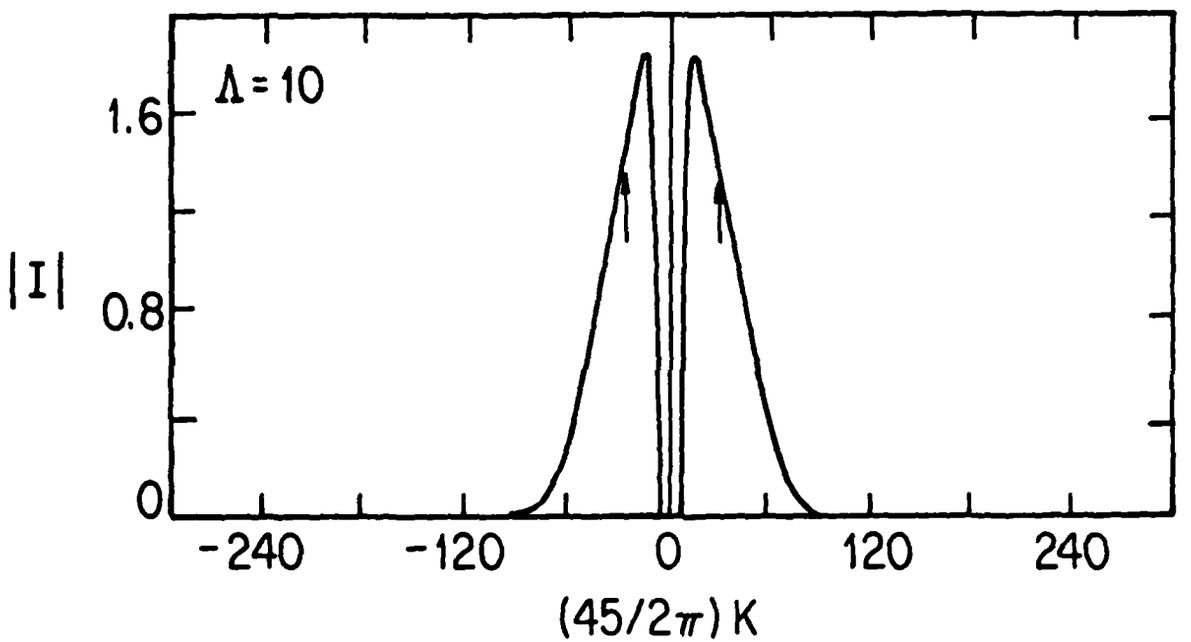
Λ = 10
1.6
0.8
0
|I|
-240
-120
0
120
240
(45/2π) K

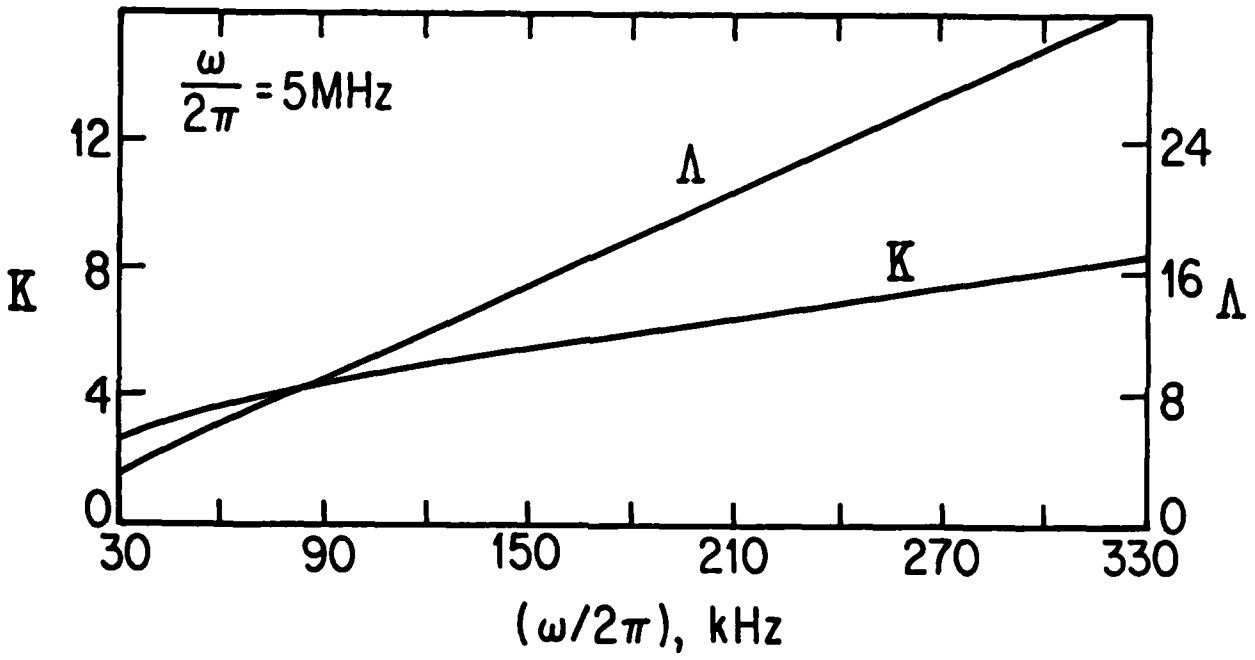
ω/2π = 5MHz
Λ
K
K
Λ
12
8
4
0
24
16
8
0
30
90
150
210
270
330
(ω/2π), kHz

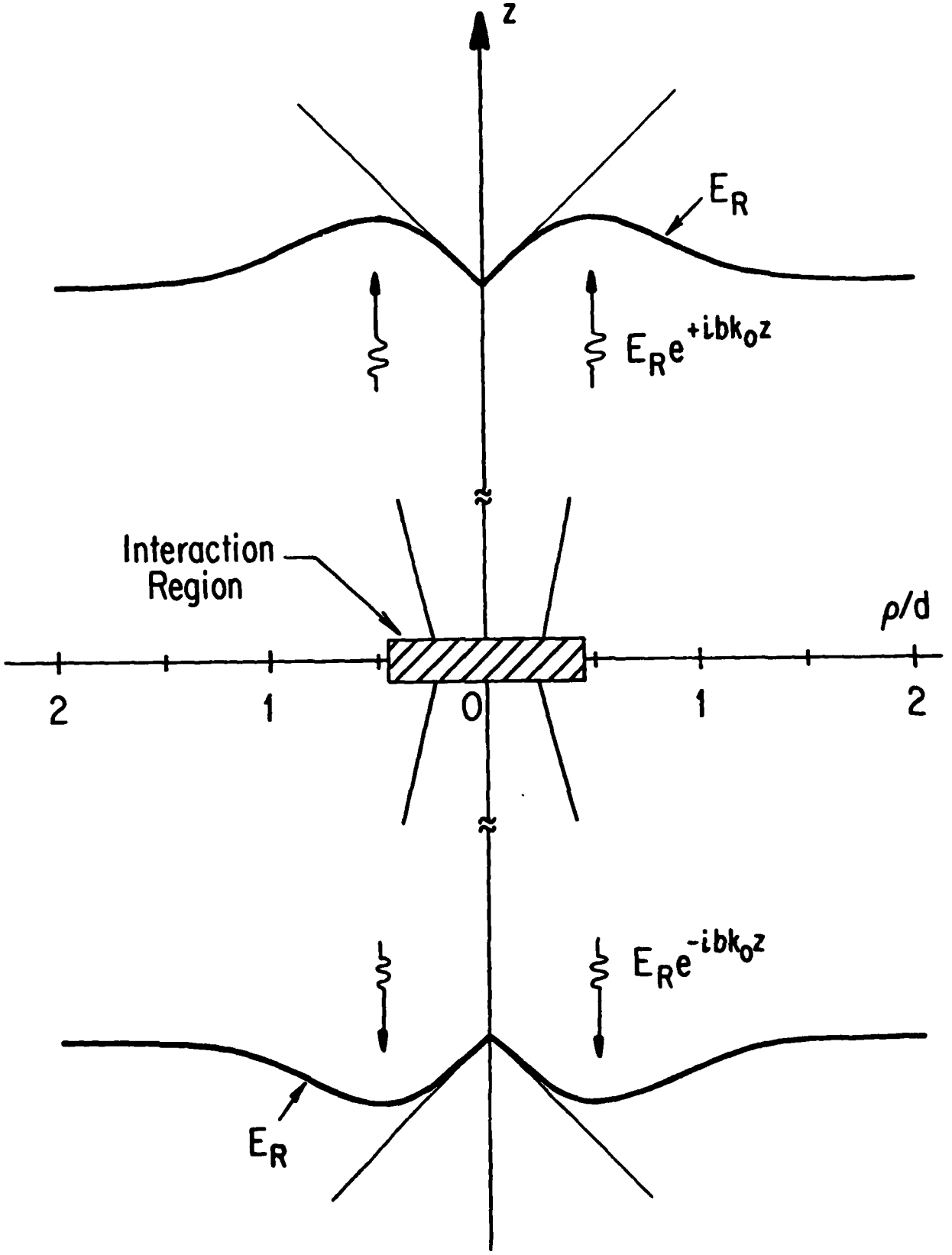
z
E_R
$E_R e^{+ibk_0 z}$
Interaction Region
ρ/d
2
1
0
1
2
$E_R e^{-ibk_0 z}$
E_R

PPG-566 "Far Infrared Laser Scattering Studies of Density Fluctuations in Tokamak Fusion Plasmas," P. Lee, N.C. Luhmann, H. Park, W.A. Peebles, R.J. Taylor, and C.X. Yu, June (1981).

PPG-567 "Energy Transport in Hot Electron Microexplosions Driven by a CO_2 Laser," C. Joshi, N.H. Burnett, and N.A. Ebrahim, June (1981).

PPG-568 "Resonance Absorption Produced Hot Electrons in a Microwave Plasma Interaction," A.Y. Lee, Y. Nishikawa, N. Luhmann, S.P. Obenschain, B. Gu, and M. Rhodes, June (1981).

PPG-569 "EXPRESS: A Computer Code to Study Helium Behavior in Inertial Confinement Fusion Reactor Structural Materials," R. Schafer and Nasr-Ghoniem, July (1981).

PPG-570 "A Note on Compton Scattering," D.D. Barbosa, July (1981).

PPG-571 "Magnetosonic Wave Heating of High Beta Plasmas," K. Nozaki, B.D. Fried, and G.J. Morales, July (1981).

PPG-572 "New York Abstracts, Papers for the New York Meeting on the Division of Plasma Physics, American Physical Society," July (1981).

PPG-573 "Energy Conservation Theorem for Electrostatic Systems," V.K. Decyk, August (1981).

PPG-574 "Finite Temperature Relativistic Magnetohydrodynamic Winds," F.S. Fujimura and C.F. Kennel, August (1981).

PPG-575 "D-D Tandem Mirror Reactor Analysis and Requirements," F. Kantrowitz and R.W. Conn, September (1981).

PPG-576 "SATYR Studies of a D-D Fueled Axisymmetric Tandem Mirror Reactor," R.W. Conn, et. al., September (1981).

PPG-577 "Observation of Mode Converted Electrostatic Waves in the ICRF Region in the Microtor Tokamak," P. Lee, et. al., September (1981).

PPG-578 "MHD Stability and Confinement in a Large Diameter, Axisymmetric Mirror with High Mirror Ratio," J. R. Ferron, A. Y. Wong, P. Young, B. Leikind, G. Dimonte, September (1981).

PPG-579 "Linear and Nonlinear Behavior of DCLC Mode in a Large Diameter, Axisymmetric Magnetic Mirror," J. R. Ferron and A. Y. Wong, September (1981).

PPG-580 "A Sufficient Criterion for Stability of Axisymmetric Collisionless Systems," A. E. Walstead, November (1981).

PPG-581 "Flute Instability in Axisymmetric Mirrors," E. A. Adler, December (1981).

PPG-582 "Efficient, Higher Order Griding Center Calculations Via the Action Form $p \cdot dq - Hdt$," R. G. Littlejohn, September (1981).

PPG-583 "Ion Heating and Confinement in the UCLA Toroidal Cusp Experiment," M. Rhodes, J. M. Dawson, J. N. Leboeuf, and N. C. Luhmann, Jr., September (1981).

PPG-584 "Laboratory Experiments on Magnetic Field Line Reconnection," R. Stenzel and W. Gekelman, October (1981).

PPG-585 "Relation of Surface Interactions to First-Wall and In-Vessel Component (IVC) Design and Materials Performance in Fusion Devices," R. Conn, October (1981).

PPG-586 "The Satyr Study of d-d Cycle Tandem Mirror Reactors," R. Conn, et al., October (1981).

PPG-587 "Assessment of Ferritic Steels for Steady-State Fusion Reactors," N. Ghoniem, R. Conn, October (1981).

PPG-588 "Mission, Concept, and Objectives of the Fusion Engineering Device (FED)," R. Conn, et al., October (1981).

PPG-589 "Studies of the Physics and Engineering of D-D Barrier Tandem Mirror Reactors," R. Conn, October (1981).

PPG-590 "Electrostatic Wave Propagation and Trapping Near the Magnetic Equator," D. D. Barbosa, October (1981).

PPG-591 "Simultaneous Observation, Spikey Turbulence and Electromagnetic Radiation," P. Y. Cheung, A. Y. Won, C. B. Darrow, S. J. Quian, October (1981).

PPG-592 "Generation of Non-Thermal Continuum Radiation in the Magnetosphere," H. Okuda, M. Ashour-Abdalla, M. S. Chance, and W. S. Kurth, November (1981).

PPG-593 "Fusion Product Energy and Particle Loss from Tandem-Mirror Reactors by Nuclear Scattering," F. Kantrowicz and R. W. Conn, November (1981).

PPG-594 "Ponderomotive Potential Near Gyroresonance," G. Dimonte, G. J. Morales, and B. M. Lamb, November (1981), submitted to Phys. Rev. Lett.

PPG-595 "Resonant Self-Focusing of Laser Light in a Plasma", C. Joshi, C. Clayton, and F. Chen, November (1981).

PPG-596 "Radiation by Runaway Electrons," M. Thaker, J. N. Leboeuf and T. Tajima, November (1981).

PPG-597 "Hamiltonian Perturbation Theory in Noncanonical Coordinates," Robert Littlejohn, November (1981).

PPG-598 "Escape of Heated Ions Upstream of a Quasi-Parallel Shock," J. P. Edmiston, C. F. Kennel and D. Eichler, Nov. (1981).

PPG-599 "Inductive Ion Acceleration and Heating in Picket Fence Geometry: Theory and Simulations", J. N. Leboeuf, J. M. Dawson S. T. Ratliff, M. Rhodes, and N. C. Luhmann, Jr., November (1981).

PPG-600 "Singular Poisson Tensors," R. G. Littlejohn, December (1980).

PPG-601 "Simulation Studies on Stability and β Limits of EBT," Y. Ohsawa and J. M. Dawson, December (1981).

PPG-602 "The Kinetics of the Interaction Between Helium and Displacement Damage in Irradiated Materials," N. Ghoniem, Sharafat, and Mansur, December (1981).

PPG-604 "Ion Cyclotron Resonance Heating in a Strongly Inhomogeneous Magnetic Field," K. Nozaki, B. D. Fried, G. Morales, and A. Fukuyama, December (1981).

PPG-603 "Multi-Mixer Far Infared Scattering Apparatus," H. K. Park, C. X. Yu, W. A. Peebles, N. C. Luhmann, December (1981).

PPG-604 "Beat Excitation of Whistler Waves," M. Shoucri, G. J. Morales, & J. E. Maggs, January (1982).

END

DATE
FILMED

04-82

DTIC